

Prediction of ultimate moment anchorage capacity of concrete filled steel box footing

Muhammad Aun Bashir^{*1}, Hitoshi Furuuchi^{2a},
Tamon Ueda^{2a} and M. Nauman Bashir^{3b}

¹ Civil Engineering Department, Imam Muhammad ibn Saud Islamic University, Riyadh, KSA, Pakistan

² Division of Engineering and Policy for Sustainable Environment, Faculty of Engineering,
Hokkaido University, Kita 13 Nishi 8, Kita-ku, Sapporo, Japan

³ Lecturer COMSATS, Sahiwal Campus, Pakistan

(Received July 17, 2012, Revised August 22, 2013, Accepted September 03, 2013)

Abstract. The objective of the study is to predict the moment anchorage capacity of the concrete filled steel box (CFSB) as footing by using the 3D finite element program CAMUI developed by authors' laboratory. The steel box is filled with concrete and concrete filled steel tube (CFT) column is inserted in the box. Numerical simulation of the experimental specimens was carried out after introducing the new constitutive model for post peak behavior of concrete in compression under confinement. The experimental program was conducted to verify the reliability of the simulation results by the FE program. The simulated peak loads agree reasonably with the experimental ones and was controlled by concrete crushing near the column. After confirming the reliability of the FEM simulation, effects of different parameters on the moment anchorage capacity of concrete filled steel box footing were clarified by conducting numerically parametric study.

Keywords: concrete filled steel box footing; 3D FEM analysis; moment capacity; parametric analysis

1. Introduction

Earthquakes that have taken place globally over the last two decades have resulted in an increased expectation of acceptable performance and damage control for different structures during seismic events. Catastrophic failures of piled foundation systems in the recent earthquakes of Loma Prieta, Northridge (Mizuno 1987, Nogami 1987, Sheppard 1983), and Kobe (Building Research Institute 1996) have led to considerable effort being directed towards safer civil infrastructure particularly in the seismic zones. However, repair of damaged piles in high-rise building systems is impractical because of the expensive cost and difficulty associated with ground excavation. In the aftermath of many earthquakes, numerous engineering inspections and investigations have been performed to assess the degree of structural damage and to evaluate the

*Corresponding author, Assistant Professor, E-mail: aunbashir@yahoo.com

^a Ph.D.

^b Ph.D. Student: E-mail: naumanuet@yahoo.com

performance of various construction materials. Most of the reports, however, address only the upper structure of buildings or bridges; very little information is available on the performance of under ground structures such as pile foundation systems and their response to earthquakes. Other studies pertain to concrete piles, yet again research work specific to performance of piles and their connection to pile cap is also very limited. Research work by Pam and Park (1990) has provided a starting point regarding the design and detailing of pile-to-pile cap connections. Specific investigation into the damage of piled foundations after earthquakes has seldom been conducted because it requires excavation and is thus costly. Past experience has shown poor connection detail of some reinforced concrete piles and hollow prestressed concrete piles performing poor seismic performance of the current pile foundation system particularly at the pile-to-pile cap connection (PPC). Lack of careful detailing and poor confinement of core concrete appears to be the reason for the failure of most of the piles. Therefore, there are still many questions left to ponder and be answered to assist the understanding of the pile-to-pile cap behavior. Potential inelastic damage has occurred at the interface between pile heads and pile cap as evidenced in recent earthquakes. It should be noted that because of the difficulties associated with the repair of foundation damage occurring during severe earthquakes, it is desirable to design the piles to remain undamaged. Therefore, damage due to recent earthquakes has resulted in an increased conservatism in the design of piles and pile-to-pile cap connections. In contrast, current recommendations produce connection detailing which result in high levels of congestion of steel reinforcement in pile cap, which make extremely difficult to construct according to designer's recommendation (Teguh *et al.* 2006).

By considering this point, a new type of footing, concrete filled steel box (CSFB) connection as footing, is presented. Steel concrete sandwich structure is a relatively new form of structural system. This form of structure has the potential to fully utilize strength of both steel and concrete with help of composite action such as confinement. It allows the prefabrication of large section in a factory, and enables rapid installation into main structure, dramatically reducing the fabrication cost and construction time. Steel faces act as permanent formwork during the construction and provide impermeable skins for the structure upon completion. So after considering these points, we selected steel box filled with concrete for isolated type of footing and pile footing. It has advantage over steel structure because of cost factor and it is a better option as compared to reinforced concrete connection due to strength and construction time.

Our purpose in this study is to develop design method for the CSFB footing by using a 3-D nonlinear finite element program CAMUI, which the authors' group has developed (Takahashi *et al.* 2005). Therefore we can take part in the development of simple and economical hybrid structure with excellent mechanical properties.

Because of the good features with the CSFB connection, it was adopted for an integrated bridge abutment which connects steel beams and foundation piles in the actual highway bridge in Sapporo, Japan (see Fig. 1). The research on this CSFB connection was started by Emoto *et al.* (2006) and continued by Bashir *et al.* (2008). The concrete filled steel box is a type of sandwich structure; however its failure mechanism is quite different from ordinary sandwich members. The major finding through both experimental and 3D-FEM numerical study by Emoto *et al.* (2006) was that failure of this connection occurs, when compression softening of concrete is caused by bearing stress from the steel pile. And other findings on shear connector effects was that the shear connector along the inserted length of pile enhanced the load carrying capacity of connection but shear connectors attached on skin plate of steel box had almost negligible effect on the strength of connection.

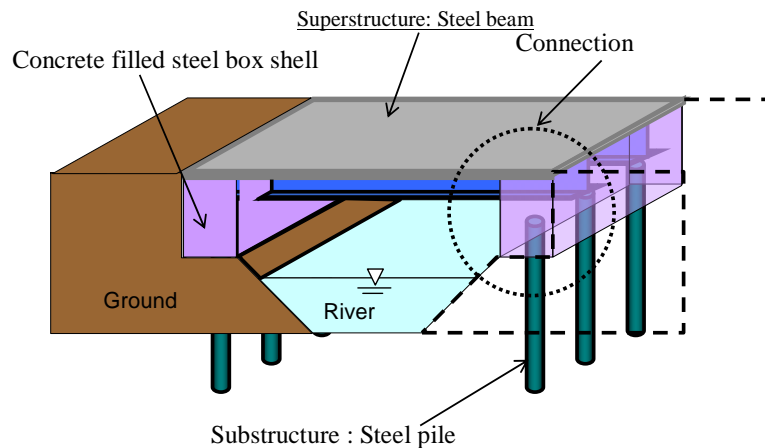


Fig. 1 Hybrid rigid frame bridge

First of all, numerical simulation, with the help of 3D non linear FEM program, of experimental specimens was carried out. The experimental program included three specimens subjected to monotonic loading perpendicular to longitudinal axis of column. The variable parameter for experimental specimens is column insertion length. Based on experimental results conclusion can be drawn that moment anchorage of footing obtained from simulation show good correlation with experimental data. After confirming the reliability of 3D non linear FEM program, parametric analysis was carried out and these parameters are insertion length, concrete strength, box size, column size, column length and box tube thickness. In this paper the effect of these important parameters are closely observed that will be useful for the development of design method of this type of footing.

2. Experimental program

Experimental program was carried out to conduct the reliability of the program for moment capacity.

2.1 Specimens

The notations A1, A2 and A3 will be used for the specimens. The principal variable of the test specimens was insertion length of the pile. The details of experimental specimens are given in Table 1. The column size and material strength were the same for all the specimens. Fig. 2 presents the dimension of the tested specimens. Bending moment was applied through the inserted pile. The inner pile was mortar filled circular steel tube, while the outer pile was circular steel tube. The concrete filled steel box together with the inserted inner pile was prepared first and the outer pile was set after wards. The gap between the inner and outer pile was carefully filled by mortar. In order to assure easy handling when the pile was fixed at the target location in the steel box, we introduced the outer pile. The steel box was fixed by the connected steel beam which was fixed at its end. Material properties are given in Table 2.

Table 1 Specimen details

Specimens	Insertion length (mm)	Box width (mm)	Steel box tube thickness (mm)	Pile diameter (mm)
A1	63.8	342.8	3.2	114.3
A2	97.8	342.8	3.2	114.3
A3	142.8	342.8	3.2	114.3

Table 2 Material properties

Specimens	Concrete strength (N/mm ²)	Concrete poisson ratio	Concrete tensile strength (N/mm ²)	Steel pile yield strength (N/mm ²)	Steel poisson ratio
A1	19.7	0.21	1.7	388.2	0.29
A2	19.7	0.21	1.7	388.2	0.29
A3	18	0.21	1.6	388.2	0.29

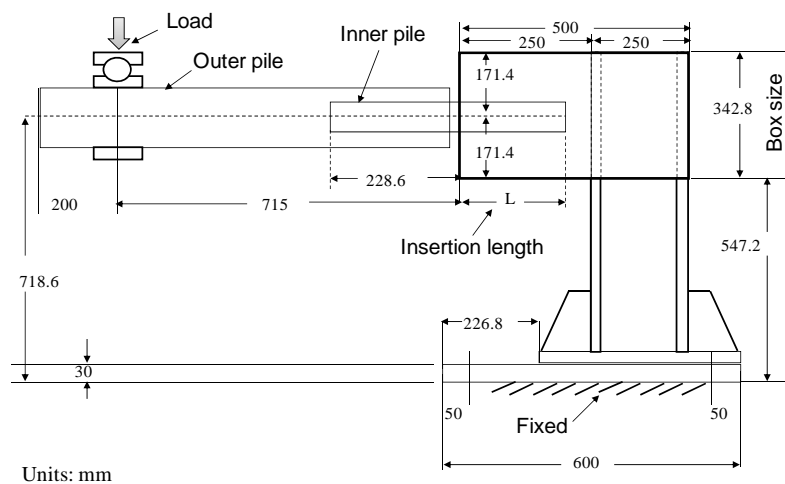


Fig. 2 Test set up and specimen details

2.2 Test set up

The specimens were placed in such a position so that the pile was horizontal and steel beam was vertical as shown in Fig. 2. Monotonic downward vertical loading was applied to the pile at different pile length. Pile length is the length of pile outside the box up to the loading point. Steel beam was fixed at the bottom. Vertical displacement of pile and steel box was measured by using the displacement transducers as shown in Fig. 3. Strain gauges were attached to the pile inside the box and outside the box as shown in Fig. 3. Spacing between the strain gauges is 20 mm.

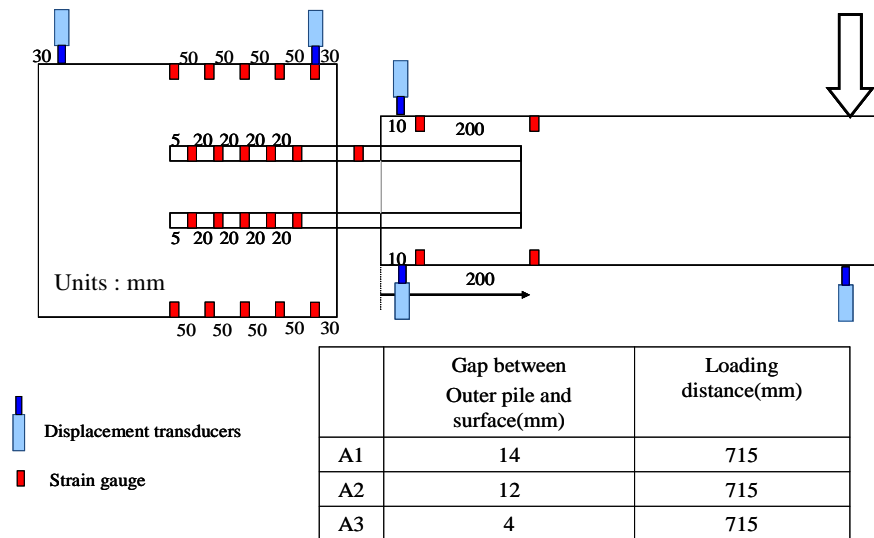


Fig. 3 Location of strain gauges and displacement transducers

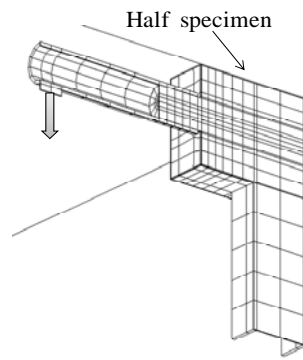


Fig. 4 Analytical specimens

3. FEM analysis

3.1 Analytical specimens

Same numbers of analytical specimens as those of the experimented specimens are prepared. The footing was symmetric, so in order to reduce the calculation time, half of the experimental specimen is modeled (see Fig. 4). 3D nonlinear finite element program CAMUI, developed by author’s laboratory, was used to analyze the specimen.

3.2 Constitutive model of materials

For un-cracked concrete and steel, elasto-plastic fracture model (Okamura and Maekawa 1991) is used. The elasto-plastic fracture model divides concrete nonlinearity into continuum damage and plasticity, and this model is also very suitable for steel. The adopted failure criteria that acted in

agreement with Niwa's model (Takahashi *et al.* 2005) in tension-compression zone and Aoyagi and Yamada's model (Takahashi *et al.* 2005) in tension-tension region were extended to three-dimensional criteria by satisfying boundary conditions (Okamura and Maekawa 1991). For cracked concrete until peak, Vecchio and Collins model (Takahashi *et al.* 2002) is used but for post peak, fracture energy equation modified by Bashir *et al.* (2010) was used. When crack occurs, a local coordinate system based on each crack plane is defined. In the case of 2 cracks occurring, two local coordinate systems arranged to share a parallel axis at the intersection line between the two crack planes. Constitutive models are applied in the direction parallel as well as normal to the crack and to shear slip along the crack planes. Global stresses are calculated by superposing the stress calculated in each local coordinate.

The tension model is expressed as following relationship between σ , the tensile stress carried by concrete and δ , the crack opening displacement.

$$\frac{\sigma}{f_t} = \left\{ 1 + \left(c_1 \frac{\delta}{\delta_0} \right)^3 \right\} \exp \left(-c_2 \frac{\delta}{\delta_0} \right) - \frac{\delta}{\delta_0} (1 + c_1^3) \exp(-c_2) \quad (1)$$

where

- c_1 : Constant 3.00 (in normal concrete)
- c_2 : Constant 6.93 (in normal concrete)
- δ_0 : Limit crack opening, 0.140 mm
- f_t : Axial tensile strength of concrete

The Vecchio and Collins model was applied for two dimensional concrete model in a plane parallel to the crack. This model is expressed as the relation between principal stress and principal strain. Compressive strength is reduced according to magnitude of tensile strain in the direction parallel to crack.

$$\sigma = f'_c \left[2 \left(\frac{\varepsilon}{\varepsilon_0} \right) - \beta \left(\frac{\varepsilon}{\varepsilon_0} \right) \right] \quad \text{for } \varepsilon < \varepsilon_p \quad (2)$$

where

- $\varepsilon_p = \varepsilon_0 / \beta$
- $\beta = 0.85 + 0.27 \varepsilon_t / \varepsilon$
- ε_t : Tensile strain in orthogonal to crack
- ε_0 : Strain at compressive strength ($2f'_c/E_c$)

For post peak, modified fracture energy equation developed by Bashir *et al.* (2010) was used.

$$G_{fc} = 8.8 \times (f'_{cc})^{0.86+7f_l/f'_c} \quad (3)$$

where

- f'_{cc} : Confined concrete stress determined by Richart *et al.* (1928).
- f_l : Lateral confining stress (average of two lateral stresses from 3D analysis).

Eq. (3) is modified form of Nakamura's equation (1999). The limit strain for compression is calculated from Nakamura *et al.* (1999).

$$\varepsilon_u = \frac{2G_{fc}}{\sigma_{peak} \times l_{eq}} + \frac{\varepsilon_p}{2} \quad (4)$$

$$\sigma = \sigma_{peak} \left[\frac{\varepsilon - \varepsilon_u}{\varepsilon_u - \varepsilon_d} \right] \tag{5}$$

where

- ε_p : Compressive strain at peak stress.
- $\sigma_{peak} = f'_{cc}/\beta$ (β was already explained in Eq. (2))
- $l_{eq} =$ Equivalent length, 40 mm which is element size.

3.3 Bond link element

Friction between steel and concrete was expressed by the bond link element with 16 nodes and 4 gauss point. The thickness of the element is considered zero. The following relationship of shear stress-slip of the friction taken from the result of the punching shear test by Inomata *et al.* (2005) was used in the FEM analysis.

$$\tau_{max} = 0.578 \times \sigma \tag{6}$$

where

- τ_{max} : Shear stress
- σ : Normal compressive stress.

4. Numerical simulation of experimental specimen

In order to show the reliability of the FEM simulation by CAMUI, the experimental results were compared with the simulation results.

Crushing of concrete surrounding the column is the dominant factor for the failure of the all specimens as shown in Fig. 5. From Fig. 6, it can be observed that experimental and analytical load displacement relationship shows good agreement in terms of ultimate load capacity. The higher stiffness of the analytical specimens A2 and A3 in comparison with the tested stiffness is probably because of the unexpected rotation of the outer pile due to the incomplete filling between



Fig. 5 Concrete crushing

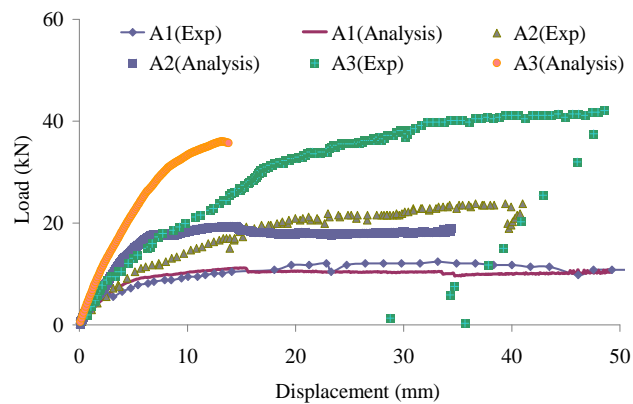


Fig. 6 Comparison of analytical and experimental results

the inner and outer pile. This difference of stiffness becomes more prominent with the increase of peak load. It was also observed that with the increase of column insertion length, the ultimate capacity of the connection increased. This increase of peak load is because of increase in resistive moment and this increase in resistive moment is explained with figure in Section 5.2.

5. Parametric study on moment anchorage capacity of concrete filled steel box footing

The effects of various parameters on the ultimate moment capacity of the concrete filled steel box as column anchorage is clarified by conducting the numerical parametric study with the FEM simulation.

5.1 Specimen details

The analytical specimens were footings which comprises of concrete filled steel tube (CFT) column inserted in concrete filled steel box and was fixed at bottom. Analytical models, as shown in Fig. 7 were prepared by using commercially available software (3D Sigma). The specimen is symmetric, so in order to reduce the mesh number, one half of the specimen was modeled. In one analysis one parameter is variable and the rest of the parameters are kept constant. The details of all the analytical specimens for footing are given in Table 3.

5.2 Effect of insertion length

In order to see the effect of insertion length on the strength of connection, four cases with different insertion length were analyzed. The insertion length for these cases was 160 mm, 200 mm, 210 mm and 260 mm respectively. After the analysis, it was observed that anchorage capacity of the footing increases with the increase of insertion length as seen in Fig. 8. This increase of peak

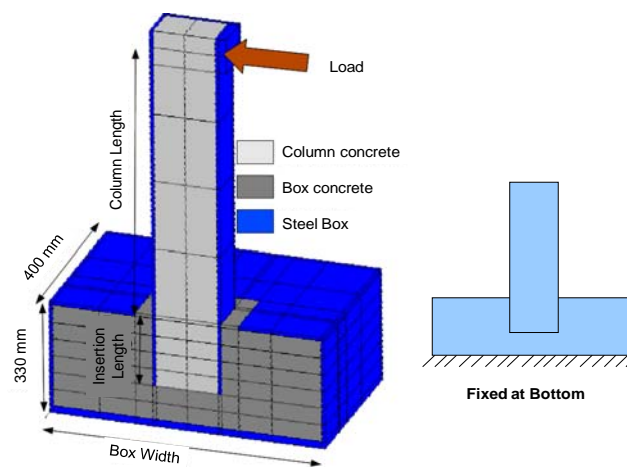


Fig. 7 Specimen details for concrete filled steel box footing connection of column

Table 3 Specimen details for parametric study on moment anchorage capacity of concrete filled steel box footing connection

Analytical specimen	Insertion length (mm)	Concrete strength (N/mm ²)	Steel box thickness (mm)	Steel box size (mm)	Column size (mm)	Column length (mm)
1	160	24	10	800	200 × 200	800
2	200					
3	210					
4	260					
5	210	18	10	800	200 × 200	800
6		24				
7		36				
8		48				
9	210	24	5	800	200 × 200	800
10			10			
11			15			
12	210	24	10	400	200 × 200	800
13				600		
14				800		
15				1200		
16	210	24	10	800	150 × 150	800
17					200 × 200	
18					250 × 250	
19	210	24	10	800	200 × 200	400
20						800
21						1200
22						1600

load is because of the increase in resistive moment. Resistive moment increases with the increase of resistive force and moment arm. The increase in resistive force is because of the increase in bearing area of concrete in which compression crushing takes place and bearing area is increased due to increase in length. Moment arm is also increased due to increase of insertion length. Increase of resistive force and moment arm can be seen in Fig. 9.

5.3 Effect of concrete strength

In order to see the effect of concrete strength on the strength of connection, four cases with different concrete strength were analyzed. The compressive strength of concrete for these cases was 18 MPa, 24 MPa, 36 MPa and 48 MPa respectively. After the analysis, it was observed that anchorage capacity of the footing increases with the increase of concrete strength as seen in Fig. 10. This increase of peak load is because of the increase in peak stress with the increase in concrete strength.

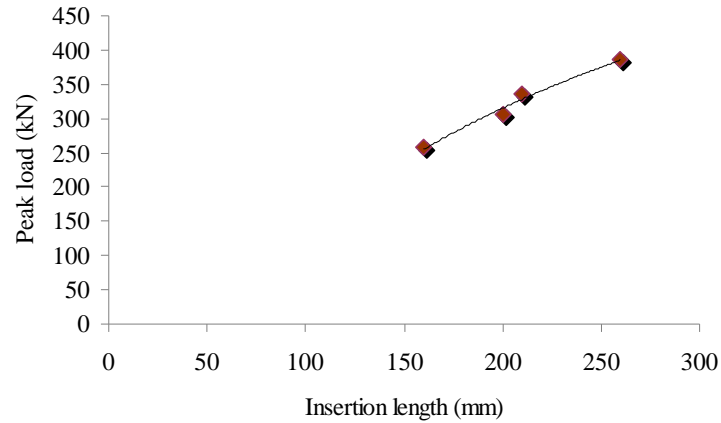


Fig. 8 Relationship between peak load and insertion length

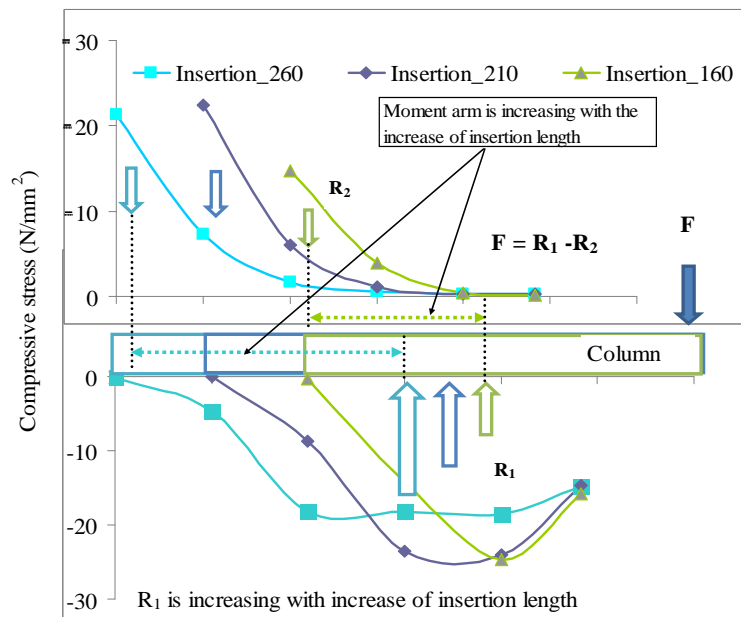


Fig. 9 Stress distribution around pile

5.4 Effect of column size

In order to see the effect of column size on the strength of connection, three cases with different column sizes were analyzed. The column sizes for these cases were (150 × 150) mm, (200 × 200) mm and (250 × 250) mm respectively. After the analysis, it was observed that anchorage capacity of the footing increases with the increase of column size as seen in Fig. 11. This increase of peak load is because of the increase in bearing area of concrete where crushing in compression takes place.

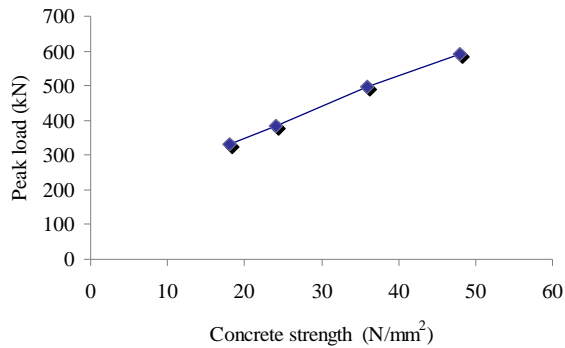


Fig. 10 Relationship between peak load and concrete strength for moment anchorage

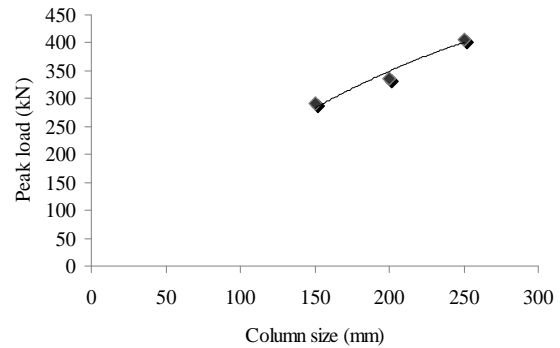


Fig. 11 Relationship between peak load and column size for moment anchorage

5.5 Effect of box size

In order to see the effect of box size on the strength of connection, four cases with different box width were analyzed. The ratio of width to column section size for these cases was 2, 3, 4 and 6 respectively. After the analysis, it was observed that anchorage capacity of the footing remains almost same with the increase of box width as seen in Fig. 12.

5.6 Effect of box thickness

In order to see the effect of box tube thickness on the strength of connection, three cases with different box tube thickness were analyzed. The thickness for these cases was 5 mm, 10 mm and 15 mm respectively. After the analysis, it was observed that anchorage capacity of the footing increases with the increase of box tube thickness as seen in Fig. 13. This increase of capacity is because of the better confinement of concrete surrounding the pile. Due to better confinement, peak stress is increased and as a result ultimate capacity increased. This explanation has already been clarified in the paper by Bashir *et al.* (2010).

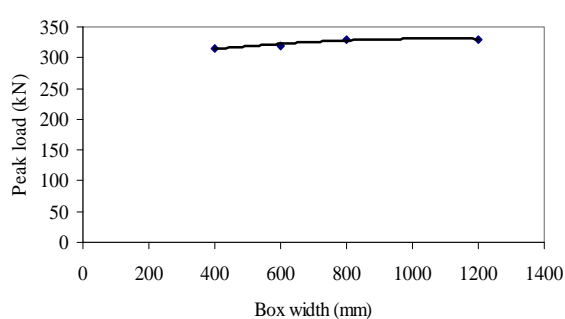


Fig. 12 Relationship between peak load and box width for moment anchorage

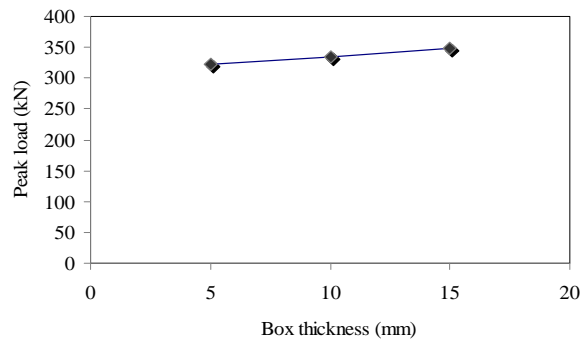


Fig. 13 Relationship between peak load and box thickness

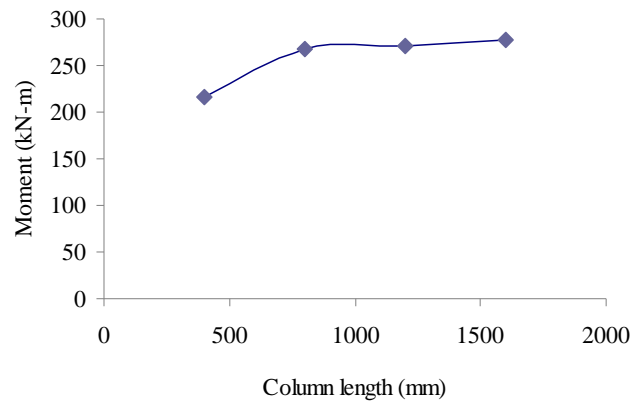


Fig. 14 Relationship between moment anchorage and column length

5.7 Effect of column length

Since the loading point of the CFT column is at its end, a longer column gives a greater ratio of bending moment to shear force in the column at the location where the column insertion starts. In order to see the effect of column length on the strength of connection, four cases with different column length were analyzed. The column length, outside the footing, for these cases was 400 mm, 800 mm, 1200 mm and 1600 mm respectively. After the analysis, it was observed that for longer pile length, failure (concrete crushing around the column) takes place due to moment and for shorter pile length shear force is the dominant cause of failure. This can be observed in the Fig. 14 in which with the increase of column length, ultimate moment capacity of the connection becomes constant.

6. Conclusions

The objective of the study was to see the effects of different parameters on moment anchorage capacity of the footing connection made of concrete filled steel box (CFSB). From the analytical study, the following conclusion can be obtained.

The moment anchorage capacity of the CFSB footing connection is affected by column insertion length, concrete strength, column size and box thickness. The box size in the range dealt with in this study does not affect the moment capacity. The effect of each factor on the moment capacity is as follows:

- The moment capacity increases with the increase of column insertion length (when changed from 160 mm to 260 mm). This increase of capacity is due to increase of resistive moment provided by the surrounding concrete. Resistive moment increased due to increase of moment arm and resistive force provided by surrounding concrete. Moment arm and resistive force increased due to increase of insertion length.
- The moment capacity increases with the increase of concrete strength (when changed from 18 MPa to 48 MPa). This increase of capacity is due to increase of concrete crushing stress (peak compressive stress) as the resistive moment.

- The moment capacity increases with the increase of column size (when changed from 150×150 mm to 250×250 mm). This increase of capacity is due to increase of bearing area of the surrounding concrete.
- The moment capacity increases with the increase of box thickness (when changed from 5mm to 15 mm). This increase of capacity is because of the increase of confinement level of concrete surrounding the pile.
- For different column length outside the steel box failure of the connection takes place because of bending moment or shear force. For pile length / insertion length ratio greater than 4, the failure takes place because of moment.

Future works

The current study is limited to moment anchorage capacity only. In future, this study will be extended for axial (tensile) load by introducing proper anchorage methods, such as indentation on column surface and end plate, for inserted column.

Acknowledgments

The authors are very grateful to MEXT for the scholarship to study in Japan and the authors are also grateful to Japan Iron and Steel Federation (Education subsidy for steel structure research, 2005) for providing financial support to conduct our experimental work. The authors are grateful to Dr Yasuhiko Sato for his valuable advice towards this study and Mr. Tsutomu Kimura and Mr. Kota Nakayama for their assistance in experimental work.

References

- Bashir, M.A., Furuuchi, H. and Ueda, T. (2008), "Parametric analysis of concrete filled steel box connection by using 3D finite element analysis", *J. Struct. Eng., JSCE*, **54A**, 815-824.
- Bashir, M.A., Nakayama, K., Furuuchi, H. and Ueda, T. (2010), "Numerical simulation of ultimate capacity of steel Pile anchorage In concrete-filled steel box connection", *Proceeding of JCI*, **32(2)**, 1219-1224.
- Building Research Institute (1996), "A survey report for building damages due to the 1995 Hyogo-ken nanbu earthquake", Ministry of Construction of Japan.
- Emoto, K., Furuuchi, H. and Ueda, T. (2006), "Analytical study on connection of rigid-frame bridge", *Proceedings of JCI*, **28(2)**, 1339-1344.
- Inomata, Y., Nakajima, A., Saiki, I. and Oe, H. (2005), "Static and fatigue bonding behavior between steel and concrete under bearing force", *J. Struct. Eng.*, **52(3)**, 1083-1090.
- Li, B., Maekawa, K. and Okamura, H. (1998), "Contact density model for stress transfer across crack in concrete", *J. Faculty of Eng., University of Tokyo*, **40(1)**, 9-52.
- Mizuno, H. (1987), "Pile damage during earthquake in Japan (1923-1983)", *Proceedings of a Session of the Geotechnical Engineering Division of the American Society of Civil Engineers in Conjunction with the ASCE*, Atlantic City, New Jersey, pp. 53-78.
- Nakamura, H. and Higai, T. (1999), "Compressive fracture energy and fracture zone length of concrete", *Seminar on Post Peak Behavior of RC Structures Subjected to Seismic Loads, JCI*, **2**, 259-272.
- Nogami, T. (Editor) (1987), "Dynamic response of pile foundations – Experiment, analysis and observation," *Proceedings of a Session of the Geotechnical Engineering Division of the American Society*

- of Civil Engineers in Conjunction with the ASCE*, Atlantic City, New Jersey, April, p. 185.
- Okamura, H. and Maekawa, K. (1991), *Nonlinear Analysis and Constitutive Models of Reinforced Concrete*, Gihodo Shuppan.
- Pam, H.J. and Park, K. (1990), "Simulated seismic load tests on prestressed concrete piles and pile cap connections", *Prestressed Concrete Inst. J.*, **35**(6), 42-61.
- Richart, F.E., Brandtzaeg, A. and Brown, R.L. (1928), "A study of the failure of concrete under combined compressive stresses", *University of Illinois Bulletin*, 185, p. 105.
- Sato, Y., Tadokoro, T., and Ueda, T., (2004), "Diagonal tensile failure mechanism of reinforced concrete beams", *J. Adv. Concrete Tech.*, **2**(3), 327-341.
- Sheppard, D.A. (1983), "Seismic design of prestressed concrete piling", *Prestressed Concrete Inst. J.*, **28**(2), 20-51.
- Takahashi, R., Sato, Y. and Ueda, T. (2002), "A simulation of shear failure of steel-concrete composite slab by 3D nonlinear FEM", *J. Struct. Eng., JSCE*, **48A**, 1297-1304.
- Takahashi, R., Sato, Y., Konno, K. and Ueda, T. (2005), "3D nonlinear punching shear simulation of steel concrete composite slab," *Journal of Advanced Concrete Technology*, **3**(2), 297-307.
- Teguh, M., Duffield, C.F., Mendis, P.A. and Hutchinson, G.L. (2006), "Seismic performance of pile-to-pile cap connections: An investigation of design issues", *Electron. J. Struct. Eng.*, **6**, 8-18.